First steps with HLLMHD and PP reconstruction: Part VI

by *O. Steiner*

Part VI is a continuation of part V, where we have shown that the models with $T_{\rm eff} = 5000$ K and with $T_{\rm eff} = 4000$ K have a slowly growing instability, which becomes really apparent only with runs of 20'000 s duration and longer. Fig. 1 shows the bolometric radiative flux through the top boundary in units of $\sigma T_{\rm eff}^4$ as a function of time for the solar model d3gt57g44n59_B0_f with $\mathbf{B} = 0$ for a time span of 48'016 s. For the solar model, nothing suspicious happens. The radiative fluctuations behave normal. Fig. 2 shows for the same run the horizontally averaged, vertical mass flux at the level of $\langle\tau\rangle = 1$ as a function of time. Here, we see that there exists a beat frequency that possibly already hints at the instability that becomes apparent in the models with $T_{\rm eff} = 5000$ K and $T_{\rm eff} = 4000$ K and which we have seen to grow in both, radiative and mass flux in part V of this report.

job	solver	reconstr.	$\nu_{\rm Smag.}$	$\nu_{\rm art.}$	$B_{\rm init}$ [G]	initial model	$t_{\rm end}$ [s]
job_d3gt57g44n59_B0_f	HLLMHD	FRweno	0.0	0.0	$B_z = 0$	d3gt57g45n59.0384735_B0	48016
job_d3t40g45mm00n01_B0_f/							
PP	HLLMHD	PP	0.0	0.0	$B_z = 0$	d3t40g45mm00n01.1320402_B0	48008
FRweno	HLLMHD	FRweno	0.0	0.0	$B_z = 0$	d3t40g45mm00n01.1320402_B0	48008
FRweno_radc	HLLMHD	FRweno	0.0	0.0	$B_z = 0$	d3t40g45mm00n01.1320402_B0	48005
FRweno_p2p	HLLMHD	FRweno	0.0	0.0	$B_z = 0$	d3t40g45mm00n01.1320402_B0	48008
vl	HLLMHD	VanLeer	0.0	0.0	$B_z = 0$	d3t40g45mm00n01.1320402_B0	40008
FRweno_RK	HLLMHD	FRweno	0.0	0.0	$B_z = 0$	d3t40g45mm00n01.1320402_B0	48013
FRweno_closedb1	HLLMHD	FRweno	0.0	0.0	$B_z = 0$	d3t40g45mm00n01.1320402_B0	38411
FRweno_closedb2	HLLMHD	FRweno	0.0	0.0	$B_z = 0$	d3t40g45mm00n01.1320402_B0	48008
FRweno_closedb3	HLLMHD	FRweno	0.0	0.0	$B_z = 0$	d3t40g45mm00n01.1320402_B0	58418
FRweno_pchange_0p1	HLLMHD	FRweno	0.0	0.0	$B_z = 0$	d3t40g45mm00n01.1320402_B0	13602
FRweno_pchange_0p6	HLLMHD	FRweno	0.0	0.0	$B_z = 0$	d3t40g45mm00n01.1320402_B0	36808
FRweno_pchange_0p8	HLLMHD	FRweno	0.0	0.0	$B_z = 0$	d3t40g45mm00n01.1320402_B0	35207
FRweno_pchange_1p0	HLLMHD	FRweno	0.0	0.0	$B_z = 0$	d3t40g45mm00n01.1320402_B0	48013

Table 1: Simulation runs carried out for part V. For job_d3t40g45mm00n01_B0_f/FRweno_radc, the Courant numbers for the radiation transfer were set C_radCourant = 0.8 and C_radCourantmax = 1.0, while these values were 2.4 and 2.6, respectively, for all other runs. For run job_d3t40g45mm00n01_B0_f/FRweno_p2p, the p2p viscosity was set c_visp2pcoeff = 0.2 and c_visp2phypsmagorinsky = 0.2. These values were zero for all other runs.

We have carried out a number of simulations with varying numerical parameters with the aim to find a remedy for this instability. These runs are summarized in Table 1. We have concentrated on the model with $T_{\rm eff} = 4000$ K, which shows the instability best.

First, we ran the model d3t40g45mm00n01 with $\mathbf{B} = 0$ using PP and VanLeer reconstruction (runs job_d3t40g45mm00n01_B0_f/PP and job_d3t40g45mm00n01_B0_f/vl) and found the same behavior as with FRweno (job_d3t40g45mm00n01_B0_f/FRweno), which was already discussed in part V. Thus, the instability grows irrespective of the reconstruction scheme. Next, we run a job with FRweno but reduced the radiative Courant number C_radCourant from 2.4 to 0.8 and C_radCourantmax from 2.6 to 1.0. This resulted in roughly twice the number of time steps but did not suppress the instability, which therefore seems not be due to the radiative time step.

Next, we changed the time integration scheme from Hancock to second order

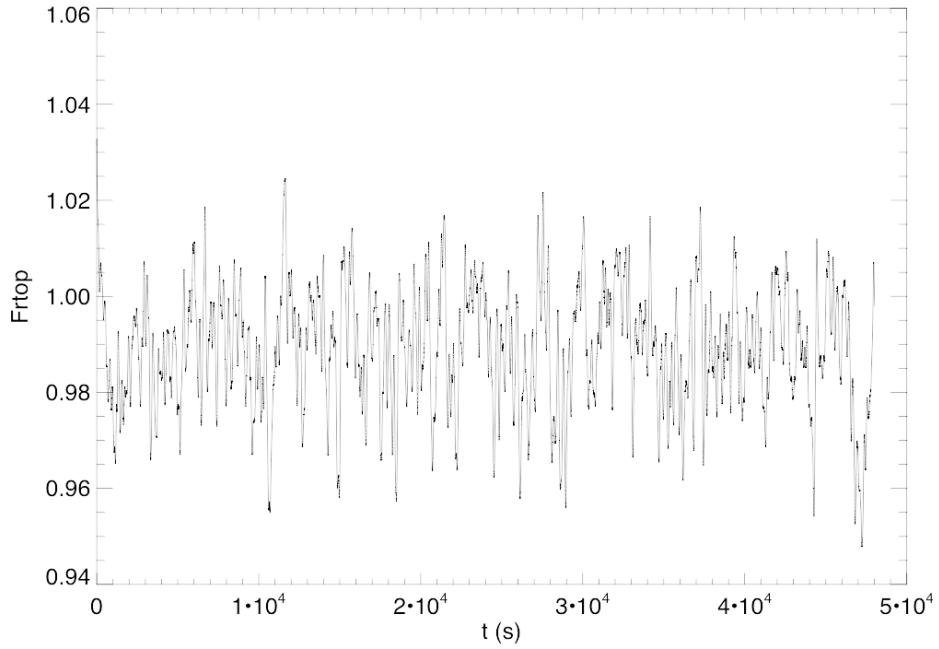

Figure 1: Bolometric radiative flux through the top boundary, Frtop, in units of $\sigma T_{\rm eff}^4$ as a function of time for the solar model d3gt57g44n59_B0_f with $\mathbf{B} = 0$ for a time span of 48'016 s. FRweno reconstruction scheme.

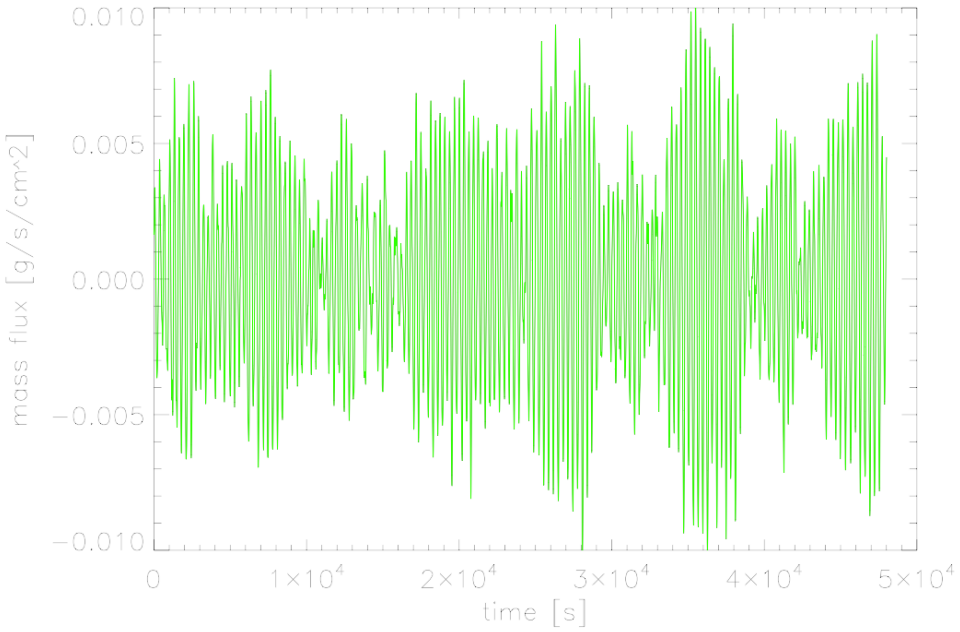

Figure 2: Horizontally averaged, vertical mass flux at the level of $\langle\tau\rangle = 1$ as a function of time for the same run as shown in Fig. 1.

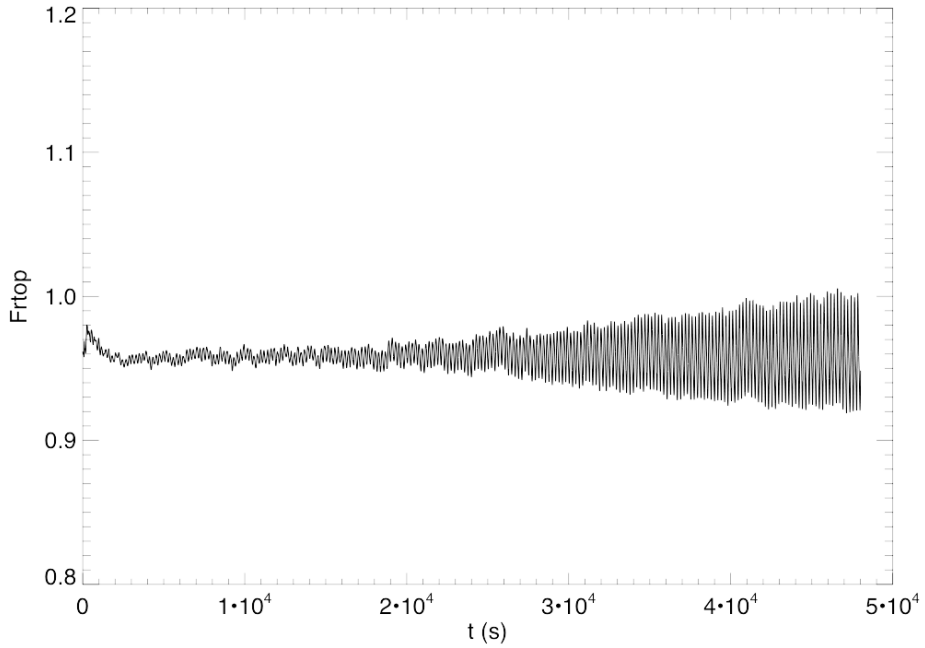

Figure 3: Bolometric radiative flux through the top boundary, Frtop, in units of $\sigma T_{\rm eff}^4$ as a function of time for the stellar model with $T_{\rm eff} = 4000$ K and $\mathbf{B} = 0$ computed with the FRweno reconstruction scheme and closed bottom boundary conditions as specified with job_d3t40g45mm00n01_B0_f/FRweno_closedb1. To be compared with Fig. 20 of part V of this report.

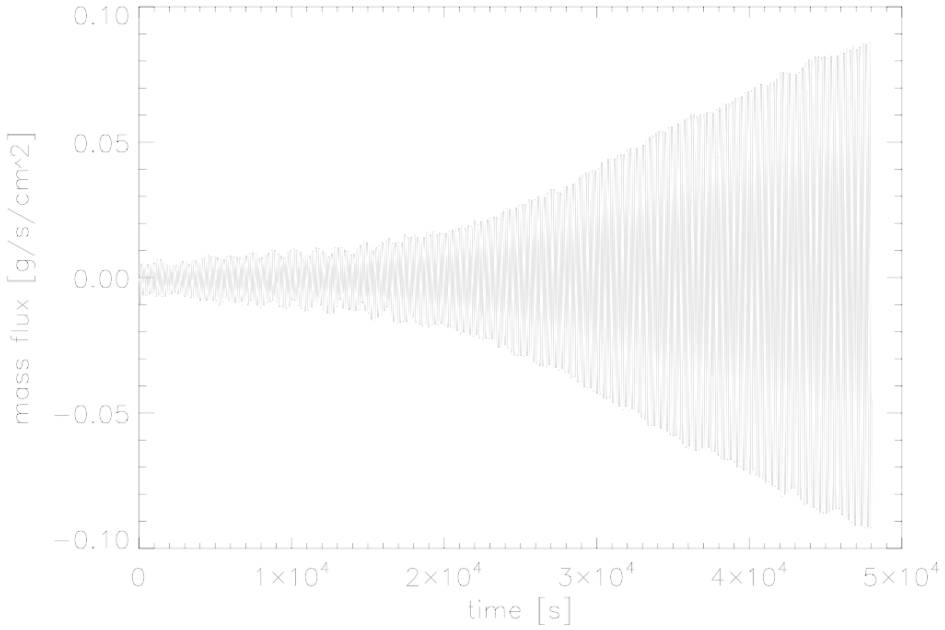

Figure 4: Horizontally averaged, vertical mass flux at the level of $\langle\tau\rangle = 1$ as a function of time for the same run as shown in Fig. 3. To be compared with Fig. 21 of part V of this report.

Runge Kutta using the FRweno reconstructtion scheme (job_d3t40g45mm00n01_B0_f/FRweno_RK). Again, no appreciable improvement. Then we invoked the P2P viscosity by setting C_visP2Pcoeff = 0.2 and C_visP2PhypSmago = 0.2. Also P2P viscosity did not have mitigating effect on the instability.

Motivated through a hint by Bernd Freytag, who suspects gravity modes at the origin of the instability, I did three runs with a closed bottom boundary. This was achieved by setting r0_grav = 6.0E+06 (instead of 1.0) and bottom_bound = closed-bottom (instead of inoutflow2). Additionally two new parameters were introduced: the parameter heat_mode, which was assigned the character string bottom_entropy2 and c_coredrag, which was set to 0.015.

This immediately had a strong effect but it did not remove the instability entirely. Fig. 3 shows the bolometric radiative flux through the top boundary as a function of time for the stellar model with $T_{\rm eff} = 4000$ K and $\mathbf{B} = 0$ computed with the FRweno reconstruction scheme and closed bottom boundary conditions with corresponding parameters as specified above. The instability still grows from the beginning but the growth rate is smaller more uniform than when computed with open bottom conditions (see Fig. 20 of part V for comparison. The horizontally averaged, vertical mass flux at the level of $\langle\tau\rangle = 1$ is shown in Fig. 4. It grows to an amplitude similar to the old run with open bottom but in a much more uniform way.

I ran two other jobs with a closed bottom boundary but with different parameter values. In job_d3t40g45mm00n01_B0_f/FRweno_closedb2 we had r0_grav = 1.2E+07 and c_coredrag = 0.03. Thus, we extended the bottom layer of the heat source and increased the damping of the flow within this layer. This solution still looked very similar to that of job_d3t40g45mm00n01_B0_f/FRweno_closedb1. Further increasing c_coredrag to a value of 0.5, finally stopped the growth of the instability as can be seen from Figs. 5 and 6. In fact, it seems that the oscillation amplitude unabatedly decreases with time.

Of course, we do not want to use the closed bottom condition for local stellar models the behavior found with this condition clearly demonstrates that the bottom boundary condition is crucial with regard to the long term instability that we discovered in part V of this report. Therefore, we now turn back to the model with an open lower boundary but change the parameter c_pchange, which controls the adjustment of the gas pressure in the bottom layers towards the global average. So far, we always had c_pchange = 0.3. Changing this parameter to 0.1 (job_d3t40g45mm00n01_B0_f/FRweno_pchange_0p1) aggravates the instability problem. The result is shown in shown in Figs. 7 and 8. While the instability started drastically to grow only after about 20'000 s in FRtop when c_pchange = 0.3, here it starts already after 5'000 s.

Next, we then increased, not decreased, the parameter c_pchange, setting it to c_pchange = 0.6. This had immediately a positive effect, regarding the instability. The results are shown in Figs. 9 and 10. The oscillation amplitude of the radiative output and the mass flux are still growing but much less dramatically than with c_pchange = 0.3, rather like with the closed bottom boundary condition and strong damping c_coredrag. Thus, we further increased c_pchange to 0.8 and further to 1.0. The results for c_pchange = 1.0 are shown in Figs. 11 and 12. Note that the scaling of the ordinate is different from Figs. 3 to 10.

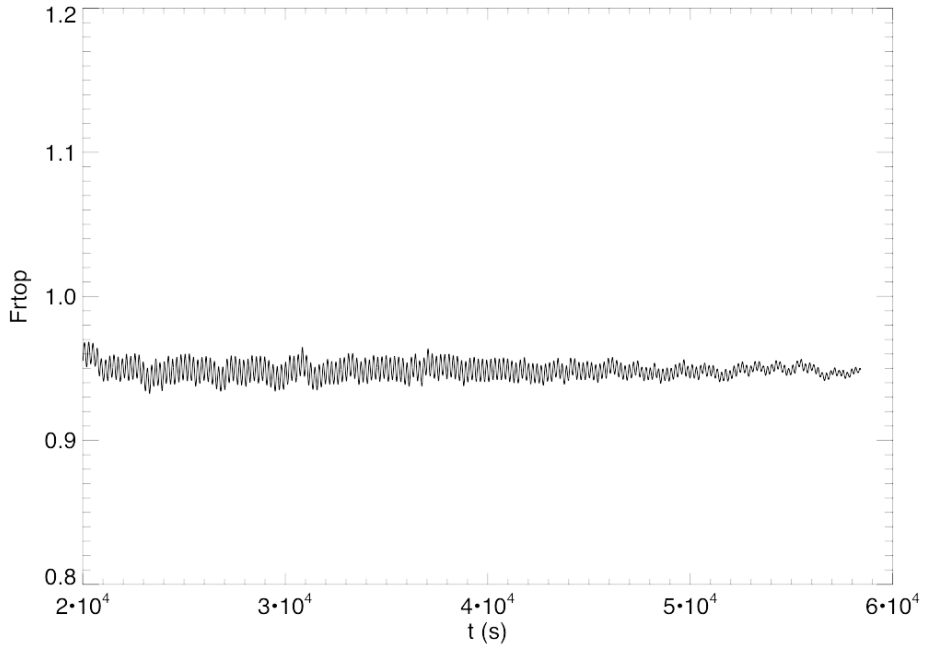

Figure 5: Bolometric radiative flux through the top boundary, Frtop, in units of $\sigma T_{\rm eff}^4$ as a function of time for the stellar model with $T_{\rm eff} = 4000$ K and $\mathbf{B} = 0$ computed with the FRweno reconstruction scheme and closed bottom boundary conditions as specified with job_d3t40g45mm00n01_B0_f/FRweno_closedb3.

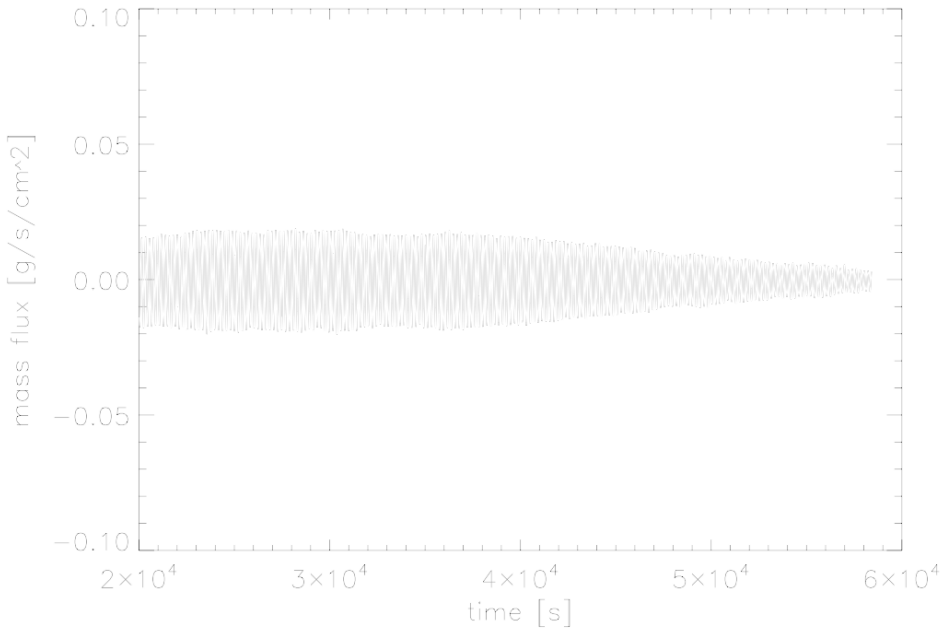

Figure 6: Horizontally averaged, vertical mass flux at the level of $\langle\tau\rangle = 1$ as a function of time for the same run as shown in Fig. 5.

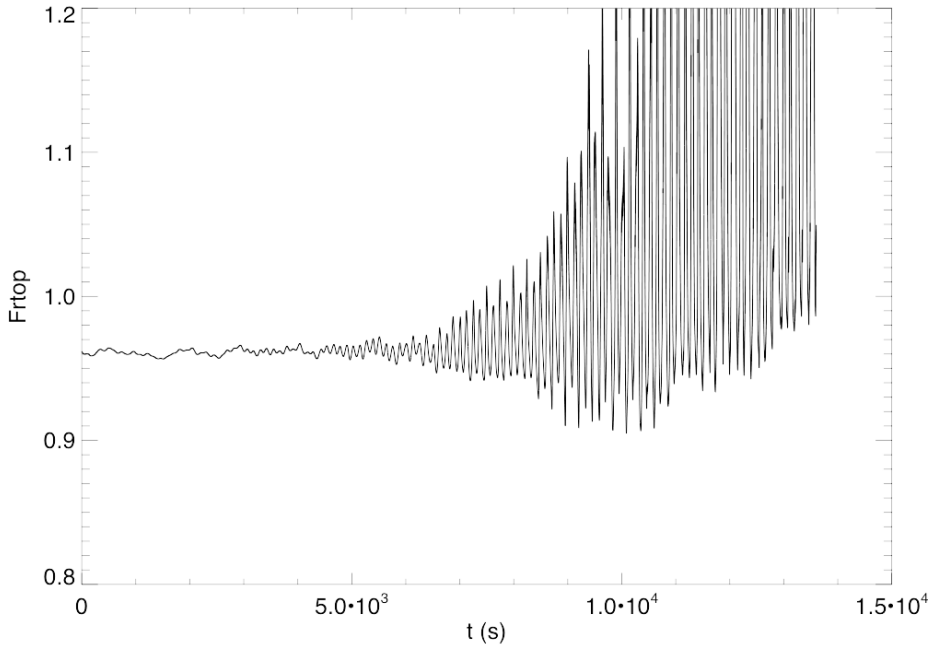

Figure 7: Bolometric radiative flux through the top boundary, Frtop, in units of $\sigma T_{\rm eff}^4$ as a function of time for the stellar model with $T_{\rm eff} = 4000$ K and $\mathbf{B} = 0$ computed with the FRweno reconstruction scheme. Parameter c_pchange = 0.1.

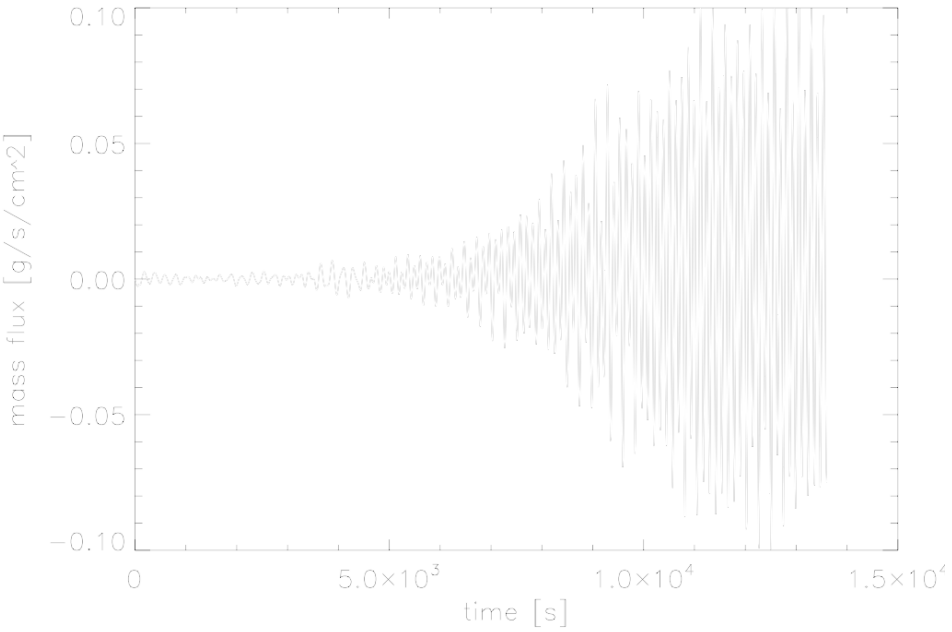

Figure 8: Horizontally averaged, vertical mass flux at the level of $\langle\tau\rangle = 1$ as a function of time for the same run as shown in Fig. 7.

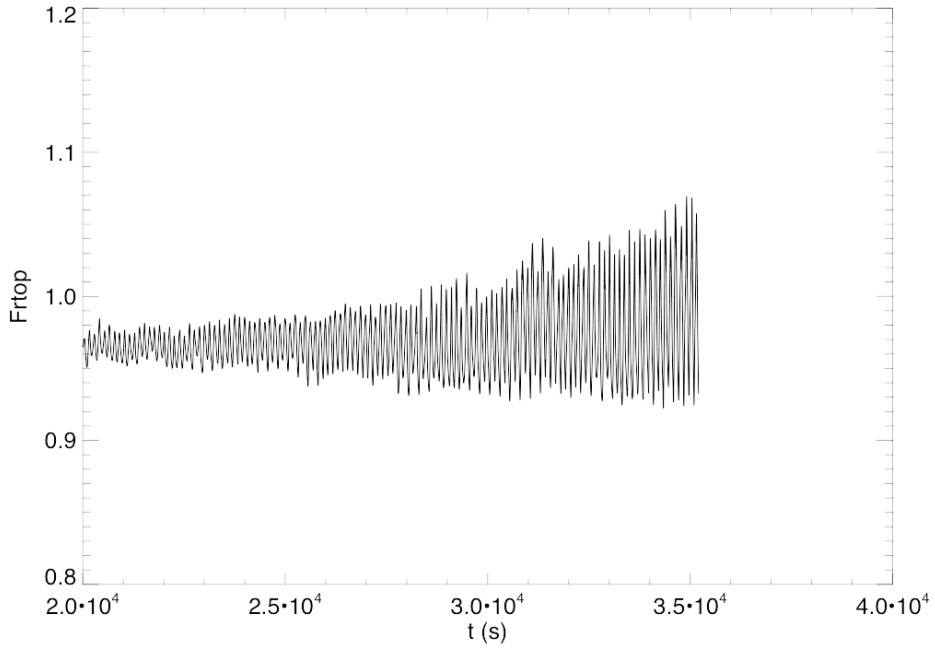

Figure 9: Bolometric radiative flux through the top boundary, Frtop, in units of $\sigma T_{\rm eff}^4$ as a function of time for the stellar model with $T_{\rm eff} = 4000$ K and $\mathbf{B} = 0$ computed with the FRweno reconstruction scheme. Parameter c_pchange = 0.6.

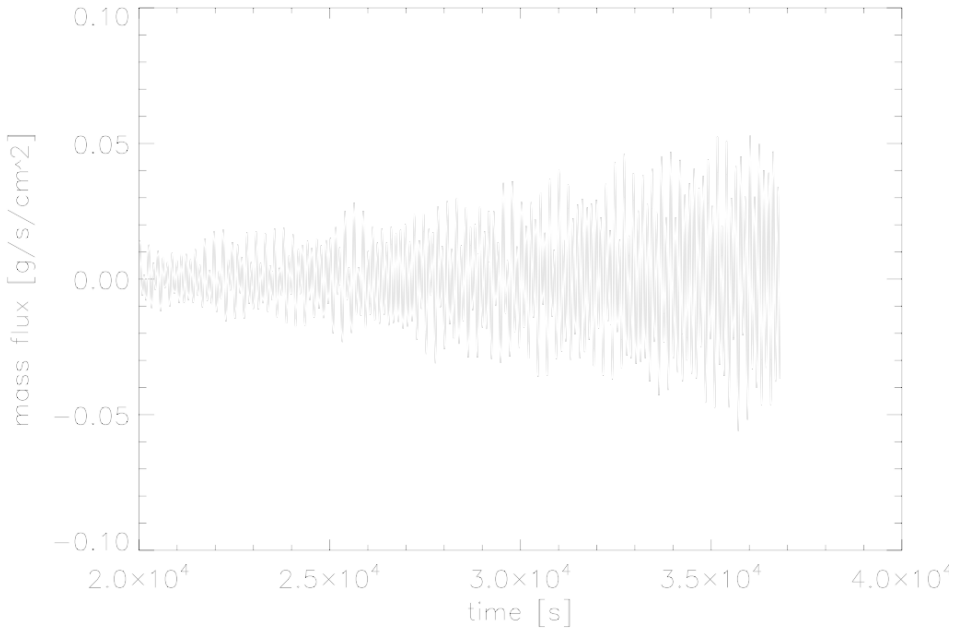

Figure 10: Horizontally averaged, vertical mass flux at the level of $\langle\tau\rangle = 1$ as a function of time for the same run as shown in Fig. 9.

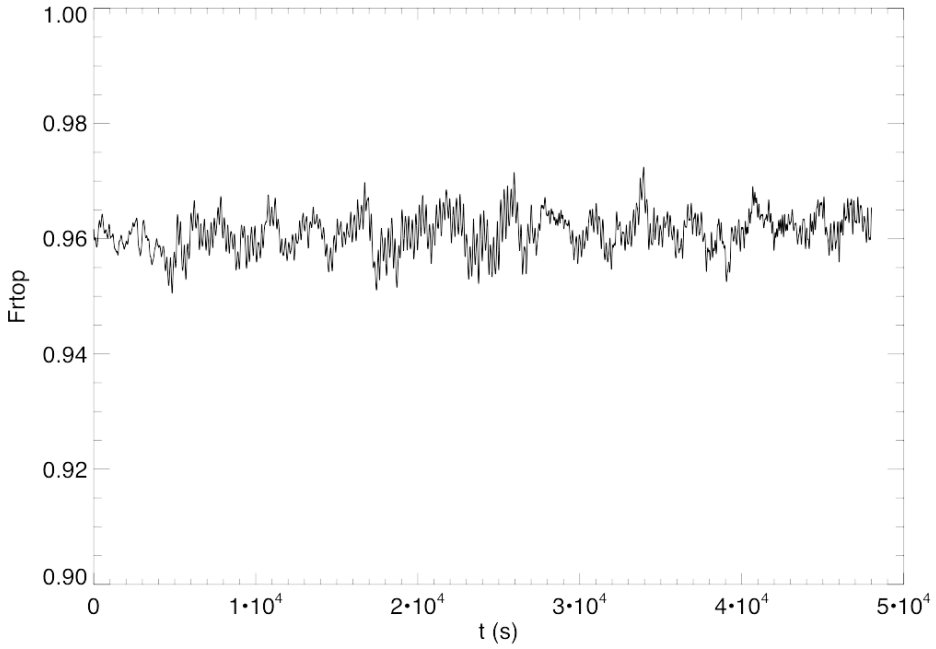

Figure 11: Bolometric radiative flux through the top boundary, Frtop, in units of $\sigma T_{\rm eff}^4$ as a function of time for the stellar model with $T_{\rm eff} = 4000$ K and $\mathbf{B} = 0$ computed with the FRweno reconstruction scheme. Parameter c_pchange = 1.0.

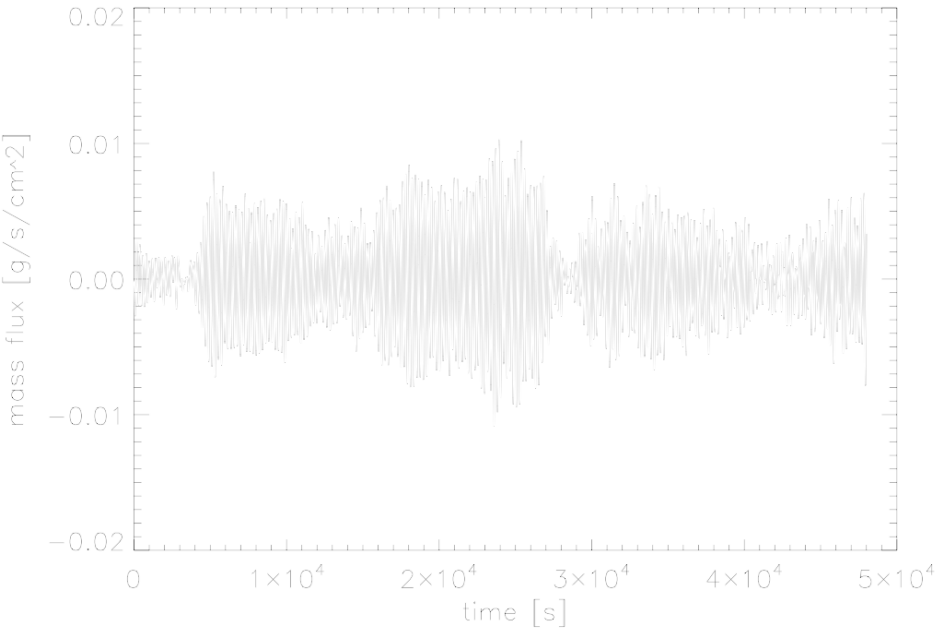

Figure 12: Horizontally averaged, vertical mass flux at the level of $\langle\tau\rangle = 1$ as a function of time for the same run as shown in Fig. 11.

At this point and time in October 2013, I thought to have solved the issue with the slowly growing instability. Setting c_pchange to 1.0 would do it. The parameter c_pchange is explained in Freytag et al. (2012, JCP 231, 919-959) Eqs. (36-37). Much later it turned out that setting c_pchange = 1.0 has detrimental consequences for properties of wave propagation in the atmosphere. The lower boundary becomes very stiff, which causes unphysical phase jumps in the propagation of pressure waves in the middle of the atmosphere. These problems are now described in an upcoming paper by Fleck, Carlsson, Khomenko, Rempel, Steiner, and Vigeesh (2020) to appear in Philosophical Transactions A. Thus, we are thrown back to square one because we better keep c_pchange = 0.3. One remedy may come with parameters C_v3ChangeLinBottom and C_v3ChangeSqrBottom which are used in subroutine rhd_bound_3DInOutFlow but not yet in rhd_bound_3DInOutFlow_mhd. But next we need to validate if the problem of the instability does still exist with the latest version of CO5BOLD.

Freiburg. i. Br., 3. 6. 2020